Al-Rafidain Journal of Engineering Sciences

Journal homepage https://rjes.iq/index.php/rjes

ISSN 3005-3153 (Online)

Thermal Conductivity of Biochar-Enhanced Sandy and Silty Soils

M. A. R. Al-Janbi[1] and A. A. Al-Obaidi[2]

[1,2] *Civil Engineering Department/ Engineering College/ Tikrit University/ Tikrit, Iraq*

a

b*dr.obaidi.a.h@tu.edu.iq*

ARTICLE INFO

Article history:
Received 08 August 2025
Revised 08 August 2025
Accepted 24 August 2025
Available online 25 August 2025

Keywords:
geotechnical backfills
biochar
pyrolysis temperature
thermal conductivity
non-cohesive soils

ABSTRACT

Near-surface soils increasingly endure vigorous thermal cycles, sharpening the need for backfills that hinder heat flow without inflating carbon footprints. This study probes biochar as a thermal modifier while deliberately varying both botanical source and pyrolysis pathway—variables seldom explored together. Seven locally abundant Iraqi woods, spanning soft to hard classes, were charred under a systematic matrix of temperatures and residence times in an oxygen-free furnace. The resulting chars were blended at graded dosages with well-graded sand and low-plasticity silt compacted to loosen, medium, and dense states, and thermal conductivity (K) was measured using a calibrated transient-needle probe. Results reveal that an intermediate-temperature pine char delivers the lowest intrinsic K and achieves pronounced insulation gains across all density states; benefits rise sharply up to about 10 wt. % dosage and level off thereafter, indicating an economical threshold for field application. By linking wood origin, , dosage, and relative density to the thermal response of sands and silts, the study furnishes a design-ready framework for climate-resilient geotechnical backfills while avoiding additional carbon burdens.

1. Introduction

Global warming is intensifying the thermal loads imposed on near-surface ground layers: the global mean surface temperature has already risen by ≈ 1.1 °C since 1851, at a rate of 0.18 °C per decade since 1981 [1]. Such accelerated warming magnifies thermal stresses on buried infrastructure; laboratory evidence shows that repeated freeze–thaw cycles alone can markedly weaken road-base layers and jeopardise long-term serviceability[2]. In this context, soil thermal conductivity (*K*) becomes a design-governing parameter for systems such as buried power cables, energy-storage layers, and sub-surface thermal barriers, where controlling heat exchange with the surrounding ground is critical [3, 4] .

Biochar produced from agricultural or woody residues has emerged as a low-carbon additive for suppressing heat flow through soils. Field trials on the North China Plain showed that applying 4.5–9 Mg ha^{-1} of corn-cob biochar reduced *K* in a wheat–maize soil by 3.5–7.5 % [5], while 30 Mg ha^{-1} of slow-pyrolysis wood char lowered *K* in cultivated loess by ≈ 25 % [6]. Laboratory studies corroborate these trends: 5 wt % corn-stalk char cut *K* of a sand by up to 35 %[7], 10 wt % rice-straw char nearly halved *K* of a red soil [8], and synergistic blends with xanthan gum further enhanced insulation while recovering strength losses [9]. The insulation efficiency of char-amended soils clearly depends on dosage, particle size, and soil fabric [10].

Corresponding author E-mail address: mahdi19aw@gmail.com
https://doi.org/10.61268/bdvj5x39

Under the current body of research, biochar's ability to curb heat transfer through soils is clear, yet sizeable blind spots persist. Botanical origin remains largely unexplored despite its potential influence. Pyrolysis settings are usually locked at one temperature and one residence time, so the combined influence of heating level and duration on char quality is still uncertain. Non-cohesive soils particularly sands and silts that dominate embankments and backfills exposed to cyclic thermal loads have likewise received scant attention.

To close these gaps, the present work produces biochar from a single, locally abundant Iraqi wood species, treats the feedstock under a systematic matrix of temperatures and residence times in an oxygen-free furnace, and blends the resulting char at selected dosages with sand and silt prepared at different relative densities. This integrated design creates a new framework for linking pyrolysis pathway to biochar properties and for evaluating their influence on the thermal behavior of non-cohesive soils in geotechnical applications.

2. Methodology

This study used two cohesionless soils from central Iraq's sand and silt. Sand and silty-clay samples were gathered from the Tigris River floodplains in Balad District, Salah al-Din Governorate, and the Al-Hawija al-Bahriya region in Dhuluiya District. Soils were recovered from 1.0–1.5 m below ground surface using a hand auger and mechanical backhoe to ensure sample homogeneity and decrease textural variability. Following ASTM D4220-14, the samples were promptly delivered to the lab in carefully sealed containers to preserve.

The pine wood was chopped into little pieces and cleansed of bark, dust, and contaminants. Air-drying in shady, well-ventilated settings for 7–10 days reduced moisture before burning. A closed, oxygen-free furnace converted pine wood into charcoal under full heat conditions, as illustrated in Figs: 1a and 1b. Experiments were done at 250°C, 550°C, and 750°C. Each condition was tested for 1.5, 3, and 6 hours. The goal was to research how temperature and time affected Biochar qualities, particularly thermal conductivity. Complete combustion of pyrolysis was used to get the lowest thermal conductivity.

Pine has the lowest heat conductivity, notably at 550°C and 3 hours. It has the lowest thermal conductivity (0.032-0.036 W/m ·K). Analyzing the findings showed that temperature was key. Decreased temperature increased thermal conductivity, whereas considerable increases, notably around 750°C, raised it again. According to the data, thermal conductivity is best around 550°C, with time having a modest influenceThe specific gravity of the biochar used in this study, determined with a water pycnometer following ASTM D854, was 1.25 . The biochar was sieved through a 0.42 mm sieve to eliminate coarse residue and guarantee consistent particle size.

2.1. Laboratory Testing The laboratory campaign comprised four groups of tests: index, engineering, chemical, and thermal. The particle-size distribution for each soil was determined in two stages. First, a sieve analysis in accordance with ASTM D6913/D6913M-17. [11]Second, the fraction passing the No. 200 sieve was examined with a hydrometer following ASTM D7928-21e1[12] . The combined gradation curves are plotted in Fig. 3. The specific gravity of soil particles (G_s) was obtained using the pycnometer method described in ASTM D854-14 [13]. The Atterberg limits were measured in accordance with ASTM D4318-17 [14] on material passing the No. 40 sieve; the resulting liquid limit (LL), plastic limit (PL), and plasticity index (PI). Minimum and maximum index densities needed to compute the relative density (Dr) were established in line with ASTM D4254-16 [15]and ASTM D4253-16[16] , respectively. The resulting maximum and minimum void ratios (e_max and e_min) and unit weights. Table 1 shows the values derived from these index tests

(a) **(b)**

Figure 1: (a) the furnace and (b) the resulting charcoal.

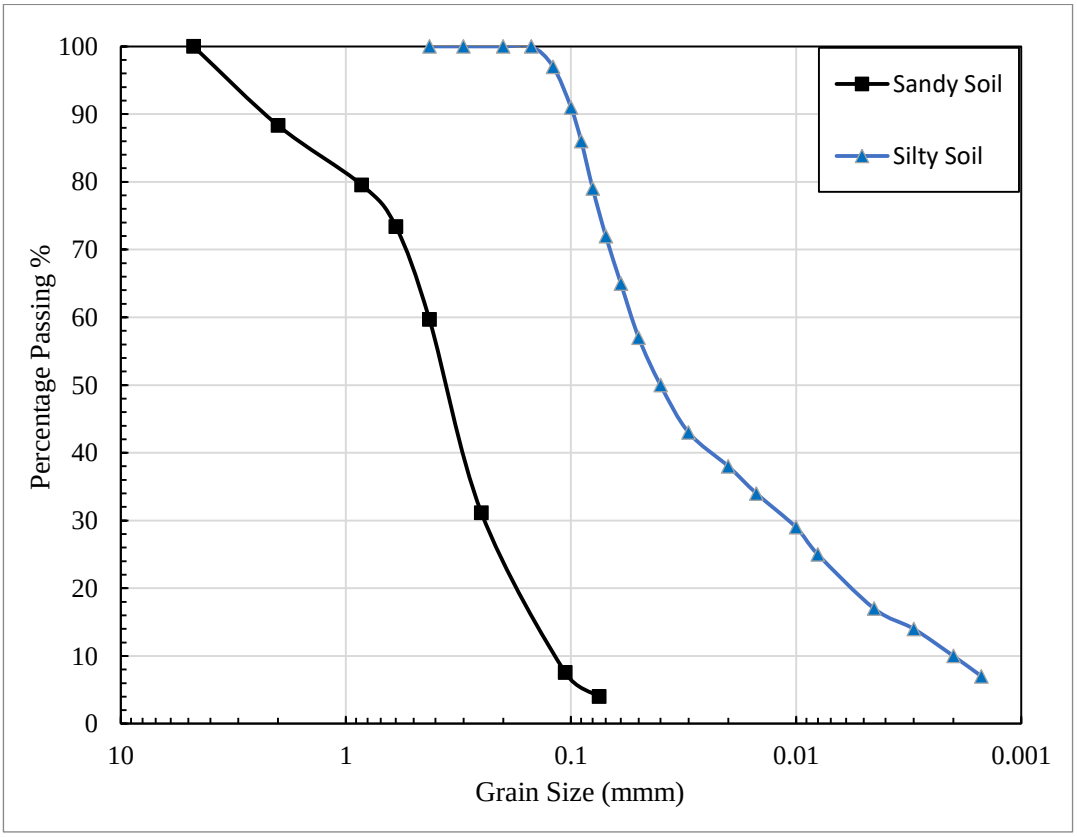

Figure 2:Grain size analysis of the soil samples

Table 1: Summary of laboratory tests performed for soil samples

Property		Sand	Silt	Specification
Soil Classification (M.I.T)	Gravel (%)	0	0	
	Sands (%)	96	25	ASTM D6913/D6913M-17
	Silts (%)	3	67	
	Clayey (%)	1	8	
D_{10} (mm)		0.116	0.003	ASTM D6913/D6913M-17 & ASTM D7928-21e1
D_{30} (mm)		0.239	0.014	&ASTM D2487-17
D_{60} (mm)		0.428	0.07	
Coefficient of uniformity c_u		3.69	23	ASTM D2487-17
Coefficient of curvature c_c		1.15	1.3	
Atterberg's Limits	Liquid Limit (%)	NP	29	
	Plastic Limit (%)	NP	25	
	Plasticity Index (%)	NP	4	ASTM D4318-17ε1 (2017)
Specific gravity G_s		2.67	2.69	ASTM D854-23
Soil Classification (USCS)	Group Symbol	SP	ML	ASTM D2487-17
	Group Name	Poorly-Graded Sand	Silt Loam	
Minimum Index unit weight (kN/m³)		15.8	13.5	ASTM D4254-23
Maximum Index unit weight (kN/m³)		19.92	16	ASTM D4253-22
e_{max}		0.627	0.75	
e_{min}		0.292	0.4	

Each soil was tested at dense, medium-dense, and loose relative densities to see how packing affected thermal–mechanical response. The relative density (Dr) of each specimen was calculated using the highest and minimum index densities from Index Tests. Dense, medium, and loose states were represented by 70%, 50%, and 28% . Table 3-2 lists sandy and silty soil dry-density limitations. Based on Lambe and Whitman (1969)[17] ranges, sand and silt samples are qualitatively dense, medium-dense, or loose., using

Table (2): Maximum and minimum dry unit weights and target relative density states for the studied sand and silt soils

Soil	sand			Silt		
γ_{dmax} (kN/m³)	19.92	19.92	19.92	16	16	16
γ_{dmin} (kN/m³)	15.8	15.8	15.8	13.5	13.5	13.5
Dr (%)	70	50	29	70	50	29
Unit weight kN/m³)	18.68	17.86	16.9	15.25	14.75	14.2
State	Dense	Medium	Loose	Dense	Medium	Loose

Table (3) Relative-density ranges and qualitative description of granular-soil state (Lambe and Whitman 1969)[17]

Relative density, Dr (%)	Description of soil
0 – 15	Very loose
15 – 35	Loose
35 – 65	Medium
65 – 85	Dense
85 – 100	Very dense

The results of Chemical Tests are shown in Table (4)

Table (4): Summary of the chemical test

Property	Sand	Silt
Organic Matter Content (OM)	0.43	0.92
Soil (pH)	8.85	9.8
Total Dissolved Solids (TDS)	0.22	0.25
Gypsum Content (%)	0.13	0.14

$$D_R\% = \left(\frac{\rho_{max} - \rho}{\rho_{max} - \rho_{min}}\right) * 100 \quad . \qquad (1)$$

Where: ρ_{dry} density of the prepared sample, ρ_{max} = maximum index density, and ρ_{min} = minimum index density

Fig. 4 shows thermal conductivity measured with a transient line-source needle probe TLS-100 per ASTM D5334-22a [18]and IEEE 442-2017. The instrument is accurate to ± 5% over 0.0001–5.0 W m^{-1} K^{-1} and has a 100 mm × 2 mm stainless-steel needle with a nichrome heater and thermistor, Al-Obaidi & Al-Karawi (2014) [19], Hoseinimighani & Szendefy (2021)[20], Schjønning (2021)[21] , and Roka et al. (2024)[22] criteria.

Biochar-Enhanced doses of 0, 5, 10, and 15% by dry mass were used to mold cylindrical specimens (150 mm height, 75 mm diameter) at dense, medium-dense, and loose relative densities. After equilibration at room temperature, the probe was inserted axially and a constant electric current was applied for ~180 s. The temperature-time curve was interpreted using the logarithmic solution from ASTM D5334 to determine thermal conductivity K and resistivity.

.

Figure 4: The device under test for one of the models

3. Results and Discussion

Thermal conductivity k was measured with the TLS-100 needle probe in accordance with ASTM D5334-22a. **Fig.5** plots k versus relative density Dr for the unamended sand and silt. In both soils k rises systematically with Dr, reflecting the progressive reduction of air voids and the increase in grain-to-grain contact as packing tightens. At any given density, the sand conducts heat more readily than the silt, a difference attributed to its coarser texture and higher quartz content.

as for the pyrolysis experiments demonstrate that pine-derived biochar produced at approximately 550 °C for three hours achieves the optimal balance of properties for thermal applications: it exhibits the lowest measured thermal conductivity (0.032 – 0.036 W m^{-1} K^{-1}), retains a highly porous carbon-rich framework that is both chemically stable and environmentally benign, and can be milled to a uniform < 0.42 mm particle size without compromising mechanical integrity. Temperatures below 550 °C leave residual volatiles that raise conductivity, whereas excessive heating (≈ 750 °C) collapses micropores and again increases k-values.These results show that controlled mid-range pyrolysis makes biochar the best insulator while keeping its light weight, ability to hold moisture, and ability to store carbon—traits that make it a great choice for long-lasting geotechnical and thermal-engineering uses .

as for the pyrolysis experiments demonstrate that pine-derived biochar produced at approximately 550 °C for three hours achieves the optimal balance of properties for thermal applications: it exhibits the lowest measured thermal conductivity (0.032 – 0.036 W m^{-1} K^{-1}), retains a highly porous carbon-rich framework that is both chemically stable and environmentally benign, and can be milled to a uniform < 0.42 mm particle size without compromising mechanical integrity. Temperatures below 550 °C leave residual volatiles that raise conductivity, whereas excessive heating (≈ 750 °C) collapses micropores and again increases k-values.These results show that controlled mid-range pyrolysis makes biochar the best insulator while keeping its light weight, ability to hold moisture, and ability to store carbon traits that make it a great choice for long-lasting geotechnical and thermal-engineering uses .

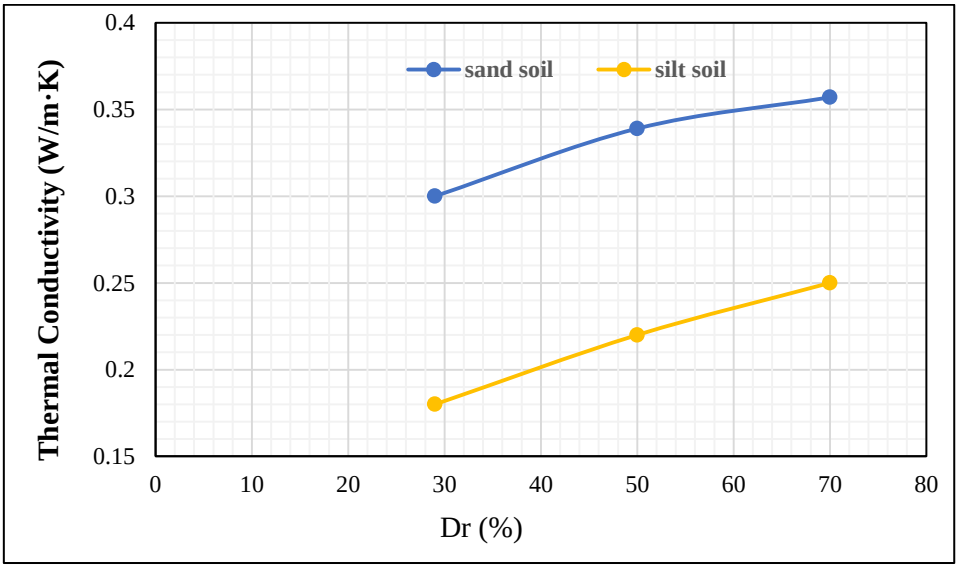

Figure 5: Thermal with relative density for sand and silt soils

3.1. Evaluation of Thermal Conductivity in Sandy Soil Amended with Biochar

The results shown in Figs 6 and 7, display the thermal conductivity curves for sand amended with biochar at three distinct dry-density states. All trajectories exhibit a progressive decline as the biochar content increases, yet the magnitude of the drop depends on the level of compaction. In the loose fabric, the curve reaches its lowest absolute value of approximately 0.12 W/mK at

15% biochar, representing an improvement of roughly 60% relative to the untreated specimen. The medium-dense and dense sands follow slightly higher, nearly parallel paths, terminating at approximately 0.157 and 0.215 W/mK, and yielding reductions of about 53% and 39%, respectively. The steepest portion of each curve lies between 0% and 10% addition, whereas the slope diminishes markedly beyond the 15% threshold, indicating a waning incremental benefit from higher dosages. The interpretation of this behavior is that the intrinsic thermal conductivity of biochar is lower than that of sand.Therefore, substituting a portion of the metallic contact points in the sand with biochar impurities disrupts the dominant solid-state conduction path through which heat is transferred. Additionally, the highly porous internal structure of biochar introduces extra air voids, increasing tortuosity and extending the effective conduction pathway. When the dosage exceeds approximately 15%, the primary intergranular conductive bridges have already been severed, and any further substitution yields only marginal benefits.

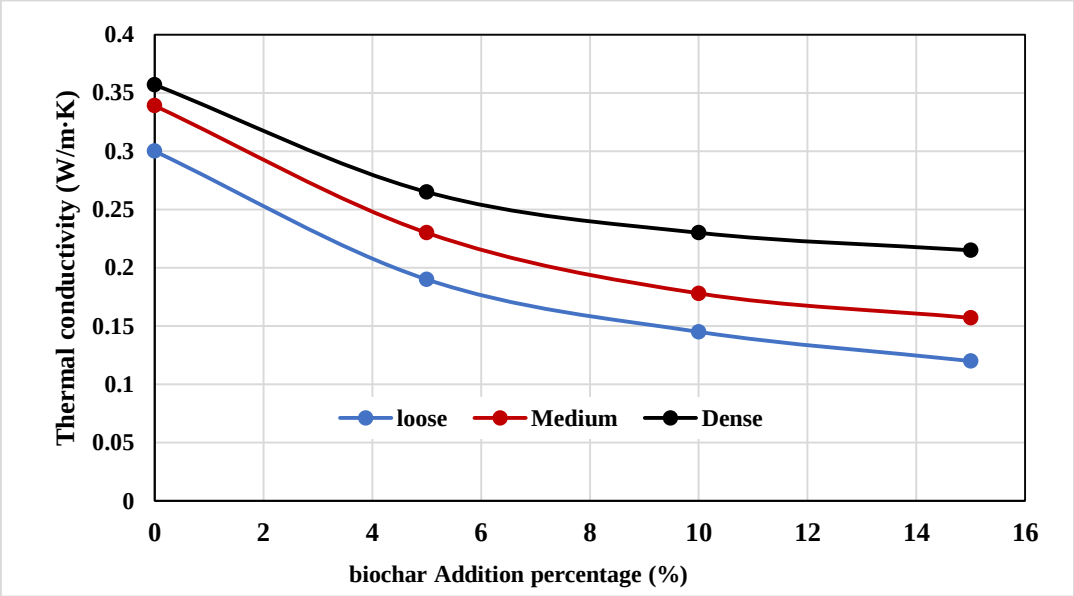

Figure 6: Relationship between thermal conductivity and biochar content in sandy soil.

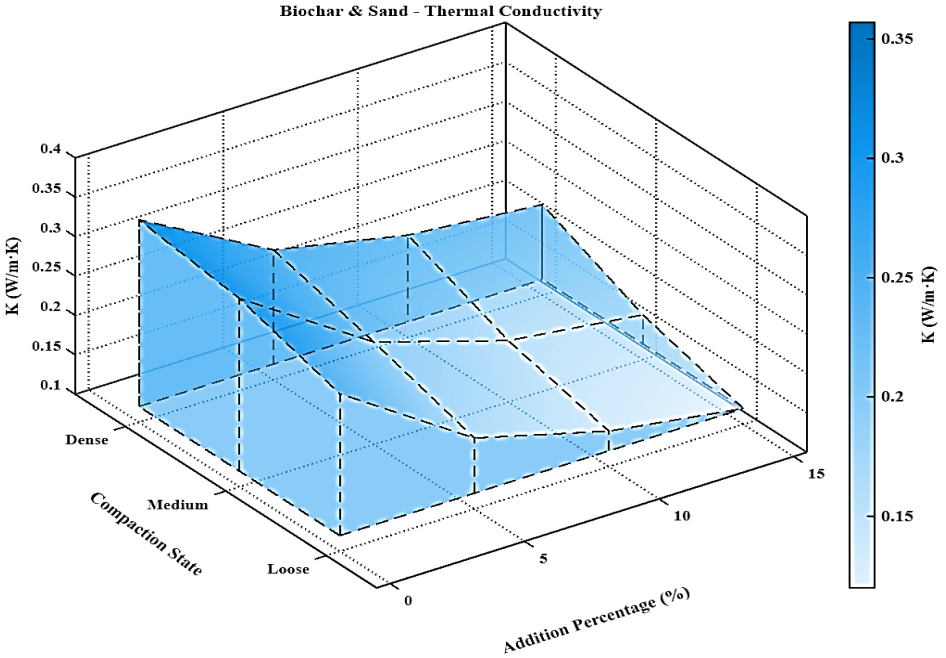

Figure 7: 3-D surface plot of thermal conductivity correlation with soil and biochar addition%

3.2. Evaluation of Thermal Conductivity in Silty Soil Amended with Biochar

Figs 8 and 9, display the thermal conductivity data for the silt soil, which clearly demonstrates a decreasing trend as the biochar concentration increases. However, the rate of decrease varies significantly depending on the extent of soil compaction. The graph shows a steep and virtually linear fall in the loose state, with an overall reduction of roughly 55% at the maximum biochar content (15%). Dense and medium-density soils, on the other hand, descend in a comparable but less noticeable manner. At the highest amount of biochar added, the medium-density state has explicitly a reduction of almost 40%, while the dense state has the lowest reduction of roughly 31%.

Advertisement. Just as shown above for sandy soils, incorporating very porous biochar into silty soil replaces many of the solid heat-transfer bridges with low-conductivity carbon. In open

samples, the higher void ratio allows biochar to drift apart, thereby elongating the conduction path and decreasing thermal conductivity to levels well beyond those of the untreated material. With larger compaction, particle interlock will effectively block the creation of new voids – and the benefits of biochar will therefore decline, until the K-dosage curve levels beyond ≈ 10 %, where excess biochar only fills available pores without creating further micro–barriers.

Biochar consistently diminishes heat conductivity in both sand and silt, with a more pronounced effect in sand. The compaction state is a crucial element, with loose mixtures exhibiting the most incredible sensitivity. This data may inform material choices for thermal management in construction.

3.3. Development of Design Charts for Thermal-Responsive Geotechnical Solutions

Previous studies demonstrate that soil temperature at depths of 30 cm or less often mirrors surface temperature due to heat penetration and thermal diffusion processes [23] [24]. Figures 7and 9 serve as design charts for thermal behavior, facilitating the quantification of heat transport in surface soil layers.

By employing Fourier's rule of heat transfer, one can leverage thermal contour shapes or isothermal profiles derived from experimental or simulated data to deduce the thickness and type of material integrated into the soil that diminishes thermal conductivity. These shapes enable the viewing of thermal gradients and the

detection of abnormalities caused by additive biochar , whose insulating properties alter the natural heat flow.

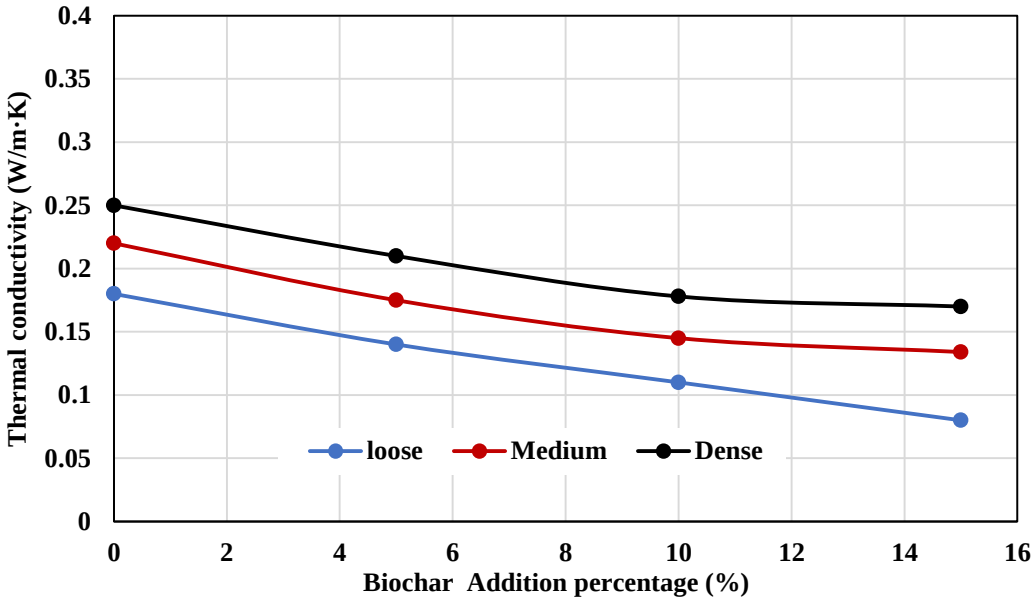

Figure 8: The relationship between thermal conductivity and biochar content in silty soil.

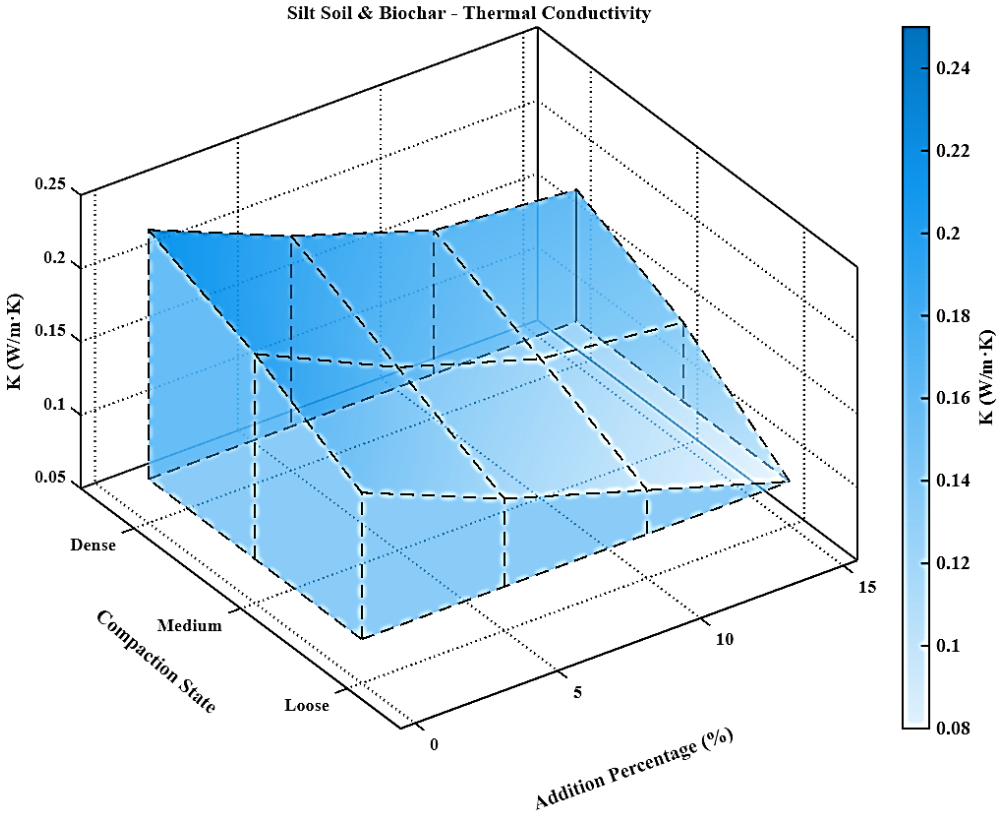

Figure 9: 3-D surface plot of thermal conductivity correlation with silty soils biochar addition%

. Consequently, the geometry of these temperature distributions can be analyzed to retrospectively ascertain the depth of the treated layer and identify the specific additive used, offering an easy approach for assessing thermal modifications in soil.

$$\frac{q}{A} = K\frac{\Delta T}{\Delta X} \qquad (1)$$

Where: q: heat flux
A: Area
K: thermal conductivity, and
(dT/dx): temperature gradient

4. Conclusion

Needle-probe readings obtained with the TLS-100 proved fully consistent with theoretical predictions and with the values reported in the literature, confirming the probe's suitability for determining the thermal conductivity of geomaterials. On this validated experimental platform, the study identified an optimum pyrolysis regime—about 550 °C for three hours—for pine wood, producing a biochar whose thermal conductivity is exceptionally low (0.032–0.036 W m^{-1} K^{-1}) and markedly superior to that of biochars derived from other feedstocks.

When this pine-derived biochar was blended into non-cohesive soils, the thermal benefit was pronounced. In loose sand, the thermal conductivity k fell from 0.30 to 0.12 W m^{-1} K^{-1}, and in loose silt from 0.18 to 0.088 W m^{-1} K^{-1}—reductions of roughly 60 % and 51 %, respectivelyThe biochar's high porosity and naturally low conductivity work together to slow down the transfer of heat through the soil matrix, which is what makes it better.

Compaction naturally diminishes void space and thus partially offsets the insulating effect, yet substantial gains are retained. At medium density, k was still reduced by about 53 % in sand and 39 % in silt; even at high density the reductions remained significant (≈ 39 % and 32 % for sand and silt, respectively). These figures demonstrate that biochar preserves a meaningful insulating capacity even in well-compacted fills typically placed around buried utilities or beneath foundations. Moreover, the data show that the most economical performance is achieved at dosages up to 10 wt %; beyond this threshold the reduction curve flattens, yielding only marginal additional benefit between 10 % and 15 %. The greatest thermal benefit is realized with additions between 0 % and 10 % by weight; beyond this point the reduction curve flattens, with only marginal gains between 10 % and 15 %. Thus, a 10 % content offers an optimal balance between performance and cost. The study therefore recommends . Long-term tests on moisture effects and freeze–thaw cycles are also advised to verify durability under changing environmental conditions. Finally, detailed investigations into the influence of mechanical mixing on strength and long-term bearing capacity should be carried out. Overall, biochar can be adopted as a low-emission thermal modifier capable of reducing soil thermal conductivity .

Acknowledgments

The authors would like to express their profound gratitude to **Dr. Azad** and his engineering team—especially **Dr. Khali‹ Dr. Tariq, Eng. Wissam, Eng. Abdulrahman, and Mr. Raad** at Andrea Laboratory—for facilitating the thermal-conductivity tests, assisting with other experimental procedures, and providing continuous technical support throughout the project.

They are equally grateful to the staff of the **Erbil Construction Laboratory**, in particular **Eng. Hassan, Eng. Alaa, Eng. Pîston, Eng. Bekrit, and Eng. Renas**, for their generous efforts in preparing the laboratory and supplying the technical assistance that enabled the structural tests.

Additional thanks go to the personnel of the engineering laboratories at **Salahaddin University, Tikrit University, and Samarra University** for their collaboration and for granting access to their facilities during various phases of the experimental campaign.

References

[1] G. Iman, "Global Temperature Graph Shows Climate Trends," Online 2021. [Online]. Available: https://www.visualcapitalist.com/global-temperature-graph-1851-2020/.

[2] S. Xiao, M. Suleiman, and M. Al-Khawaja, "Investigation of effects of temperature cycles on soil-concrete interface behavior using direct shear tests," *Soils and Foundations*, vol. 59, 08/01 2019, doi: 10.1016/j.sandf.2019.04.009.

[3] O. T. Farouki, "Thermal Properties of Soils," U.S. Army Cold Regions Research and Engineering Laboratory, Hanover, NH, 1981/12 1981.

[4] A. Moradi, K. Smits, N. Lu, and J. McCartney, "Heat Transfer in Unsaturated Soil with Application to Borehole Thermal Energy Storage," *Vadose Zone Journal*, vol. 15, 10/01 2016, doi: 10.2136/vzj2016.03.0027.

[5] Q. Zhang, T. Ren, J. Zhao, Z. Du, and Y. Wang, "Effects of biochar amendment on soil thermal properties in the North China Plain," *Soil Science Society of America Journal*, vol. 80, no. 3, pp. 719-728, 2016, doi: 10.2136/sssaj2016.01.0020.

[6] J. Usowicz, J. Lipiec, M. Łukowski, and W. Marczewski, "The effect of biochar application on thermal properties and albedo of loess soil under grassland and fallow," *Soil & Tillage Research*, vol. 164, pp. 45-51, 2016, doi: 10.1016/j.still.2016.03.009.

[7] B. Zhao, L. Li, Y. Zhao, and X. Zhang, "Thermal conductivity of a Brown Earth soil as affected by biochars derived at different temperatures: Experiment and prediction with the Campbell model," *International Agrophysics*, vol. 34, no. 4, pp. 433-439, 2020.

[8] S. Yang, S. Wi, J. Lee, H. Lee, and S. Kim, "Biochar-red clay composites for energy efficiency as eco-friendly building materials: Thermal and mechanical performance," *Journal of Hazardous Materials*, vol. 373, pp. 844-855, 2019, doi: 10.1016/j.jhazmat.2019.03.079.

[9] D. Patwa, A. A. Dubey, R. Karangat, and S. Sekharan, "Investigation of thermal and strength characteristics of a natural backfill composite inspired by synergistic biochar–biopolymer amendment of clay loam," *Canadian Geotechnical Journal*, vol. 61, 09/21 2023, doi: 10.1139/cgj-2022-0528.

[10] J. Xiong, R. Yu, E. Islam, F. Zhu, and J. Zha, "Effect of biochar on soil temperature under high soil-surface temperature in coal-mined arid and semiarid regions," *Sustainability*, vol. 12, no. 19, pp. 8238-8238, 2020, doi: 10.3390/su12198238.

[11] A. International, "Standard Test Methods for Particle Size Distribution (Gradation) of Soils Using Sieve Analysis," ASTM International, ASTM D6913/D6913M-17, 2017. [Online]. Available: https://www.astm.org/d6913_d6913m-17.html

[12] A. International, "Standard Test Method for Particle-Size Distribution (Gradation) of Fine-Grained Soils Using the Sedimentation (Hydrometer) Analysis," ASTM International, ASTM D7928-21E01, 2021.

[13] A. International, "Standard Test Methods for Specific Gravity of Soil Solids by Water Pycnometer," ASTM International, ASTM D854-14, 2014.

[14] A. International, "Standard Test Methods for Liquid Limit, Plastic Limit, and Plasticity Index of Soils," ASTM International, ASTM D4318-17, 2017.

[15] A. International, "Standard Test Methods for Minimum Index Density and Unit Weight of Soils and Calculation of Relative Density," ASTM International, ASTM D4254-16, 2016.

[16] A. International, "Standard Test Methods for Maximum Index Density and Unit Weight of Soils Using a Vibratory Table," ASTM International, ASTM D4253-16, 2016.

[17] T. W. Lambe and R. V. Whitman, *Soil Mechanics*. Cambridge, MA: MIT Press, 1969.

[18] A. International, "Standard Test Method for Determination of Thermal Conductivity of Soil and Rock by Thermal Needle Probe Procedure," ASTM International, ASTM D5334-22, 2022.

[19] A. Al-Obaidi and A. A. Al-Karawi, "Thermal conductivity of gypseous soil under different temperatures," in *11th International Congress on Advances in Civil Engineering (ACE 2014)*, Istanbul, Turkey, 2014/10 2014.

[20] H. Hoseinimighani and J. Szendefy, "Comparison of different methods for measuring thermal properties of soil: review on laboratory, in-situ and numerical modeling methods," in *6th International Conference on Geotechnical and Geophysical Site Characterization*, Budapest, Hungary, 2021/09/26 2021.

[21] P. Schjønning, "Thermal conductivity of undisturbed soil—Measurements and predictions," *Geoderma*, vol. 402, pp. 115188-115188, 2021, doi: 10.1016/j.geoderma.2021.115188.

[22] B. R. Roka, A. Vieira, A. Figueiredo, and C. Cardoso, "Measurement and comparison of thermal properties of soils in Portugal using needle and plane source methods for use in shallow geothermal energy application," in *Research Summit 2024 Book of Abstracts*, 2024, pp. 259-259.

[23] A. Sapriza, G. Gonzalo, S. Razavi, and H. Wheater, "On the appropriate definition of soil profile configuration and initial conditions for land surface–hydrology models in cold regions," *Hydrology and Earth System Sciences*, vol. 22, pp. 3295-3309, 2018, doi: 10.5194/hess-22-3295-2018.

[24] A. Al Obaidi, "Temperature variations and its effect on some engineering properties of Tikrit soils," *Scientific Journal of Tikrit University-Engineering-Sciences*, vol. 6, no. 5 Suppl., pp. 13-28, 1999.